Građevinski materijali i konstrukcije
Building Materials and Structures
journal homepage: www.dimk.rs

https://doi.org/10.5937/GRMK2300017R UDK: 691.32:620.17

Original scientific paper

Concrete crack analysis using a deep belief convolutional neural network

Geetha Ramalingam[1)], Vijayalakshmi Ramalingam[*2)], Prakash Ramaiah[3)], Sathia Ramalinam[4)]

[6)] *Department of Biomedical Engineering, Saveetha School of Engineering, SIMATS, Chennai. India*
[7)] *Associate Professor, Department of Civil Engineering, Sri Sivasubramaniya Nadar College of Engineering- India*
[8)] *Associate Professor, Department of Civil Engineering, Government College of Engineering, Tirunelveli- India*
[9)] *Associate Professor, Department of Civil Engineering Sri Venkateswara College of Engineering, India*

Article history

Received: 02 January 2024
Received in revised form: 19 February 2024
Accepted: 04 March 2024
Available online: 22 March 2024

Keywords

Machine Learning,
Convolutional Neural Network,
Concrete structure,
cracks,
Deep Neural Network,
Unsupervised Learning

ABSTRACT

The assessment of surface cracks in concrete structures plays a pivotal role in determining structural integrity. However, current diagnostic technologies suffer from drawbacks such as being time-consuming, subjective, and reliant on inspectors' experience, resulting in low detection accuracy. This paper seeks to address these issues by proposing an automated, vision-based method for identifying the surface condition of concrete structures. The method integrates advanced pre-trained convolutional neural networks (CNNs), transfer learning, and decision-level image fusion. To develop and validate this approach, a total of 6,500 image patches from diverse concrete surfaces were generated. Each pre-trained CNN establishes a predictive model for the initial diagnosis of surface conditions through transfer learning. Given the potential for conflicting results among different CNNs due to architectural differences, a modified Deep Belief CNN algorithm is crafted, thereby enhancing crack detection accuracy. The effectiveness of the proposed method is confirmed through a comparison with other CNN models. Robustness is tested by subjecting the method to images with various types and intensities of noise, yielding satisfactory outcomes. In practical scenarios, the hybridised approach is applied to analyse field-captured images of concrete structures using an exhaustive search-based scanning window. Results showcase the method's capacity to accurately identify crack profiles, with minimal areas of incorrect predictions underscoring its potential for practical applications.

1 Introduction

Cracks in concrete are a common phenomenon that may occur due to moisture movement, temperature variation, elastic deformation, creep, chemical reactions, foundation movement, and the settlement of soil. But unforeseen cracks may affect the durability and serviceability of the structure which in turn may affect its service life. Cracks in concrete occur when the strain exceeds the tensile strain capacity of the concrete [1]. For flexural members, the crack occurs on the top and bottom surfaces of the flexural member. The cracks start from the tension face and propagate to the compression zone perpendicular to the axis of the member. Widening of cracks may lead to corrosion of the reinforcement and ultimately lead to the failure of the structure [2]. Various parameters that influence the width of cracks are tensile stress in the longitudinal bars, thickness of the concrete cover, diameter and spacing of the longitudinal bars, depth of the member and location of the neutral axis, bond strength, and tensile strength of the concrete [3]. The crack width in a structural member is calculated to satisfy the limit state of serviceability. Different patterns of cracks developed in beams and columns are shown in Figures 1 and 2 respectively. Adding fibres to the concrete helps to increase the tensile strength, impact strength, strain capacity, and crack width and shrinkage. Previous research has demonstrated that adding fibres to concrete helps improve the properties of concrete in the post-cracking behaviour [4]. Fibres added to the concrete matrix improve the fracture energy, post-cracking stiffness, and ductility of the concrete rather than its strength. The tensile strength of fibres contributes mainly to improving the crack arresting mechanism of concrete in pre-cracking as well as in the post-peak region [5]. Once cracks develop in concrete, the fibres share the stress and distribute the stress across the cross section, which reduces the stress concentration and prevents the formation of wider Cracks, as shown in Figure 3. The strain redistribution across the cracks in plain concrete is achieved through bridging actions in the form of aggregate interlock. In FRC, the fibre stretching and pull-out help with crack bridging in addition to the aggregate interlock [6]. An experimentally tested specimen showing the crack width behaviours for plain concrete and fibre-reinforced concrete is shown in Figure. 4.

* Corresponding author:
E-mail address: VijayalakshmiR@ssn.edu.in

Figure 1. Cracks in structural beam member with flexural shear crack

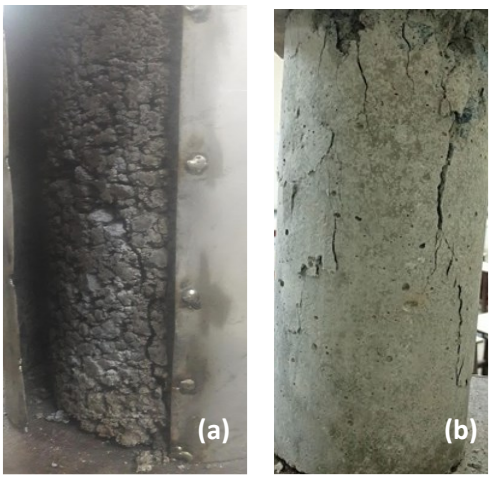

Figure 2. Cracks in column members(a) Diagonal Cracks (b) Splitting Cracks

Figure 3. Crack pattern in masonry unit without fibre and with natural fibre

Figure 4. Crack width of concrete (a) without fibres and (b) bridging of crack in fibre-reinforced concrete

Emperical formulas and equations were suggested by many codal standards, such as IS 456-2000 (equation 1-4), BS-Euro code - BS EN1992-1-1-2004 (equation 5-9), Egyptian code (equation 10-13) and American Concrete Institute ACI-code (equation 14-16). In addition, many researchers have developed an emperical model to calculate the crack width in concrete. The formulas suggested by different codes are given below.

The crack width (Wcr) formula suggested by IS 456-2000:

$$W_{cr} = \frac{3a_{cr}\varepsilon_m}{1+\frac{2(a_{cr}-c_{min})}{h-x}} \quad (1)$$

$$\varepsilon_m = \varepsilon_1 \frac{b(h-x)(a-x)}{3E_sA_s(d-x)} \quad (2)$$

$$\varepsilon_1 = \frac{Mx}{I_C(0.5E_c)} \quad (3)$$

$$I = \frac{bx}{3} + (mA_{st}(d-x)^2) \quad (4)$$

The equation for crack width as per EURO code:

$$w_k = S_{r,max}(\varepsilon_{sm} - \varepsilon_{cm}) \quad (5)$$

$$(\varepsilon_{sm} - \varepsilon_{cm}) = \frac{(f_s - k_t(\frac{ct,eff(1+n\rho_{eff})}{\rho_{eff}})}{E_s} \geq 0.6\frac{f_s}{E_s} \quad (6)$$

$$n = \frac{E_s}{E_c} \quad (7)$$

$$\rho = \frac{A_s}{A_{c,eff}} \quad (8)$$

$$S_{r,max} = 3.4C + \frac{0.425k_1k_2\emptyset}{\rho_{eff}} \quad (9)$$

The equation of crack width as per Egyptian code:

$$W_k = \beta\varepsilon_{sm}S_{rm} \quad (10)$$

$$\varepsilon_{sm} = \frac{f_s}{E_s}(1 - \beta_1\beta_2(\frac{f_{scr}}{f_s}))^2 \quad (11)$$

$$S_{rm} = 50 + 0.25k_1k_2\emptyset\rho_{eff} \quad (12)$$

$$f_{scr} = \frac{mMd_c}{I_{cr}} \quad (13)$$

The equation suggested by ACI 318-95 code:

$$W_{max} = 0.011\beta f_s\sqrt[3]{d_cA_o}10^{-3}mm \quad (14)$$

$$A_o = \frac{2d_cb}{3} \quad (15)$$

$$\beta = \frac{h-x}{d-x} \quad (16)$$

In addressing the importance of identifying structural surface cracks and recognising the limitations of existing inspection methods, both academia and industry are actively pursuing the automation of crack diagnosis with high accuracy and real-time capability. The rapid advancement of computer vision and machine learning (ML) technologies in recent years has led to the proposal of numerous automatic approaches as powerful tools to tackle the challenges of crack detection in practical applications [7]. Early research in vision-based automated crack detection primarily focused on developing algorithms for crack edge detection using image processing methods. For example, Abdel-Qader et al. conducted a performance comparison of four edge detection filters—fast Fourier transform, fast Haar transform, Canny, and Sobel—for crack detection, with results based on fifty images of a concrete bridge showing that the fast Haar transform outperformed the other three filters, demonstrating the highest accuracy in crack detection. Kim et al. investigated the parameter optimization of current binarization methods for crack detection by reducing errors between real crack widths and estimated ones [8]. Rabah et al. proposed a three-step approach, involving shade rectification, crack detection, and mapping, for detecting and mapping cracks based on terrestrial laser scanning (TLS) point cloud data [9]. In another study, Yamaguchi et al. introduced a novel percolation model to extract concrete surface cracks by considering percolated area shape and brightness connectivity [10]. The primary limitation of existing image processing-based approaches is their tendency to emphasise local patterns more than global features, despite cracks being global properties of the image. Some cracks in an image may be neglected when more attention is given to local patterns. To address this issue, several studies have started integrating image processing methods with ML technologies to enhance detection accuracy. Lee et al. initiated the utilisation of artificial neural networks to identify the length, width, and orientation of concrete surface cracks [11]. Li et al. created a new way to find concrete that uses an active contour model along with the Canny filter and support vector machine (SVM) [12]. Jahanshahi et al. utilised linear discriminant analysis (LDA) to extract features sensitive to cracks, which were then used as inputs to train three classifiers, including SVM, ANN, and nearest-neighbour [13]. In [14,15] CNN model is trained to discern the crack patterns, allowing it to forecast stress-crack correlations. Initially tailored to specific air-void configurations, it possesses the flexibility to accommodate a wider array of microstructures, thereby incorporating a broader spectrum of pore-related data. Although the combination of ML and image processing-based feature extraction has demonstrated the ability to improve crack detection accuracy, it may still encounter challenges in identifying cracks in images with complex background characteristics and noise. The main reason for this issue is that crack feature extraction is typically performed manually. While hand-crafted crack features may offer an optimal solution for a specific dataset, they may struggle to consistently perform well on a set of new crack images captured in a more intricate environment.

2 Literature review

In recent years, deep learning (DL), as a subset of machine learning (ML), has experienced rapid development, leveraging the advantage of seamlessly integrating automatic feature extraction and nonlinear classification [16]. A plethora of predictive models featuring deeper network architectures have emerged for the purpose of concrete surface crack detection. For instance, Xu et al. introduced a deep learning model comprising multiple layers of restricted Boltzmann machines for abstract feature learning, effectively identifying fatigue cracks within images featuring complex backgrounds [17]. Modarres et al. applied convolutional neural networks (CNN) to classify structural surface cracks of varying shapes and sizes, demonstrating that the performance of the trained model remains robust across different locations and pixel resolutions in images [18]. Additionally, Jo and Jadidi devised an autonomous crack classification system based on a deep belief network, trained using 15,000 infrared and RGB images with and without cracks [19]. Li and Zhao modified AlexNet to create a deep CNN model tailored for concrete crack detection, successfully incorporating it into a smartphone for practical applications [20]. Chen and Jahanshahi fused CNN with a data fusion algorithm to analyse video frames for crack detection. The proposed fusion framework aggregates features from each frame, enhancing the robustness and accuracy of the system [21]. Similar endeavours are

documented in Ref. [22], where a hybrid model comprising fully connected CNN and naive Bayes fusion was employed to recognise cracks in a concrete bridge.

In general, image-based deep learning (DL) approaches for crack identification can be classified into three groups: **Region-Based Detection:** Focuses on localising cracks within an image by generating image patches and determining whether each patch contains a crack. Preferred for automatically diagnosing the localised crack area on the surface of concrete structures. **Object Detection:** Aims to distinguish cracks from other objects using DL-based detectors. **Segmentation Methods:** Conducts pixel-level crack detection by classifying whether each pixel contains a crack or not. Each category of method has its own advantages and drawbacks. For example, while crack segmentation methods require significant computational power, region-based methods are preferred for localising crack areas on concrete structures for automatic diagnosis. Current approaches for crack region detection often utilise convolutional neural networks (CNNs) to handle image patches with pixel resolutions of 512 × 512 or 256 × 256, detecting cracks in images with larger pixel sizes. However, a limitation of this method is that the developed CNNs can only detect cracks of similar sizes as the patches. In cases where a crack has a pixel size of 32 × 32 in an image with a pixel size of 256 × 256, the trained model will consider the entire patch containing the crack, resulting in a coarse detection result. Consequently, these CNN models need to be retrained based on many image patches with smaller pixel sizes, which is computationally expensive. Figure 5 depicts the architecture of a basic CNN model.

To overcome the challenges outlined above, this research proposes an integrated method for detecting surface cracks in concrete structures with greater precision. This approach incorporates a sliding window based on an exhaustive search, pre-trained Convolutional Neural Networks (CNNs) with more complex architectures, transfer learning, and data fusion techniques. Initially, a sliding window is applied to divide the original image into smaller patches with reduced pixel resolution for crack detection. Subsequently, CNN-based classification models are established to determine whether each crack contains the defect or not. It is well recognised that the efficacy of the developed model is contingent on the quality and quantity of the training data. However, obtaining a large number of image samples with diverse crack patterns for training a deep network architecture is impractical in real-world scenarios. Alternatively, models for crack patch detection can be derived by retraining CNN models originally developed for distinct but related tasks using transfer learning. In this context, 15 pre-trained CNNs initially designed for classifying images into 1000 object categories are repurposed as models for crack patch detection. As these pre-trained CNNs exhibit varying performances due to distinct network architectures, the predictive outcomes from different models may conflict, making it challenging for the system to reach a final decision. To address this issue, a new Deep Belief CNN algorithm is devised to amalgamate the detection results from various CNN models, yielding a comprehensive assessment of the surface condition of concrete structures.

The capacity of CNNs to generalise effectively is widely acknowledged, primarily contingent on having a substantial volume of training data, especially data with clear labels. When there's a reduction in the quantity of training data, the ensuing decline in classification accuracy can lead to the challenge of overfitting. The exceptional performance of CNNs in image recognition is fundamentally linked to their training on extensive datasets. However, researchers in the engineering domain often encounter difficulties in acquiring a satisfactory amount of meaningful data. In response to this challenge, transfer learning (TL) has emerged as a robust technique. It not only diminishes the dependence of networks on the magnitude of training data but also maximises the utilisation of existing data. In contrast to conventional machine learning methods, TL categorises the dataset into source and target domains. The central tenet of TL involves applying knowledge gleaned from the source domain to address pertinent tasks in the target domain, effectively resolving issues specific to the target [23].

3 Proposed method

A Deep Belief Network (DBN) is proposed in this work, shown in Figure 6. It is a type of artificial neural network architecture. DBN consists of multiple layers of stochastic, latent variables. It belongs to the broader family of deep learning models and is particularly associated with unsupervised learning tasks. DBNs are notable for their ability to learn hierarchical representations of data and have been used in various applications, including feature learning, dimensionality reduction, and generative modelling. A typical DBN is structured as a stack of Restricted Boltzmann Machines (RBMs). An RBM is a type of probabilistic graphical model with two layers: a visible layer representing the input data and a hidden layer capturing learned features. Training a DBN involves a two-step process: pre-training and fine-tuning. Pre-training: Each RBM in the stack is trained in an unsupervised manner to capture hierarchical features.

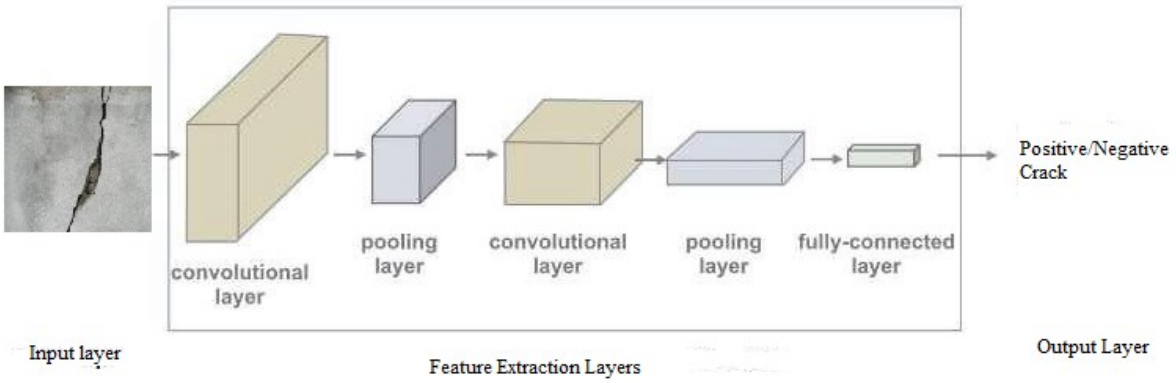

Figure 5. Architecture of a basic Convolutional Neural Network

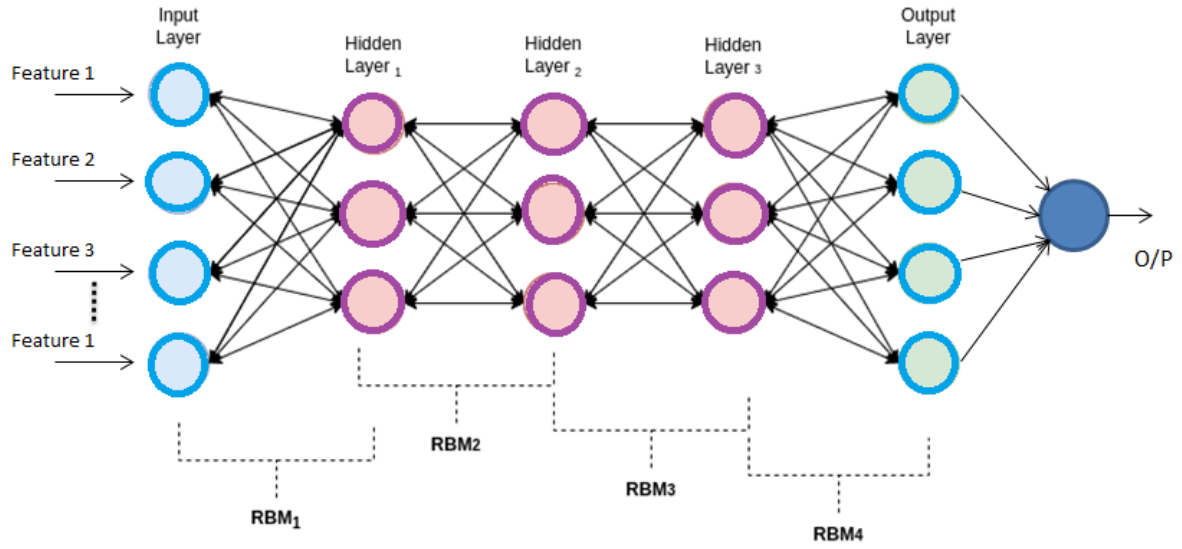

Figure 6. Deep Belief Network

This layer-wise pre-training initialises the weights of the network. Fine-tuning: The entire network is fine-tuned using supervised learning, typically using back propagation and gradient descent. DBNs can be used as generative models, capable of generating new samples similar to the training data. The RBM's capacity to learn a probability distribution over the input data facilitates this. Lower layers capture simple and local features, while higher layers represent more complex and global features, thanks to the hierarchical representation that DBNs learn. Dimensionality Reduction: DBNs can be used to reduce the dimensionality of data while retaining important features. Feature Extraction: Extracting meaningful features from raw data in an unsupervised manner. Generative Tasks: Generating new samples like the training data. Training deep networks can be computationally intensive, and fine-tuning requires labelled data for supervised learning. DBNs share similarities with deep autoencoders and deep neural networks. However, the layer-wise training of RBMs distinguishes them from some other deep learning architectures. It is important to note that while DBNs have been influential, more recent advancements in deep learning, such as deep neural networks (DNNs) and convolutional neural networks (CNNs), have gained more prominence due to their scalability and performance on a wide range of tasks. The dataset, comprising images of cracks along with their associated depth information, is inputted into a Convolutional Neural Network (CNN). Within the CNN model, the feature extraction layer processes the images, extracting pertinent features. Subsequently, these extracted features serve as input for training and testing the regression models. The integrated CNN model is employed to predict the depth of the cracks. Figure 7. depicts the flow of the developed CNN model to predict the cracks.

3.1 Boundary

DBNs are generative models and can generate new samples from the learned probability distribution. This property allows them to be used for tasks such as generating synthetic data or filling in missing values. DBNs are adept at learning hierarchical representations of the input data, capturing both low-level and high-level features in a distributed manner across the layers.

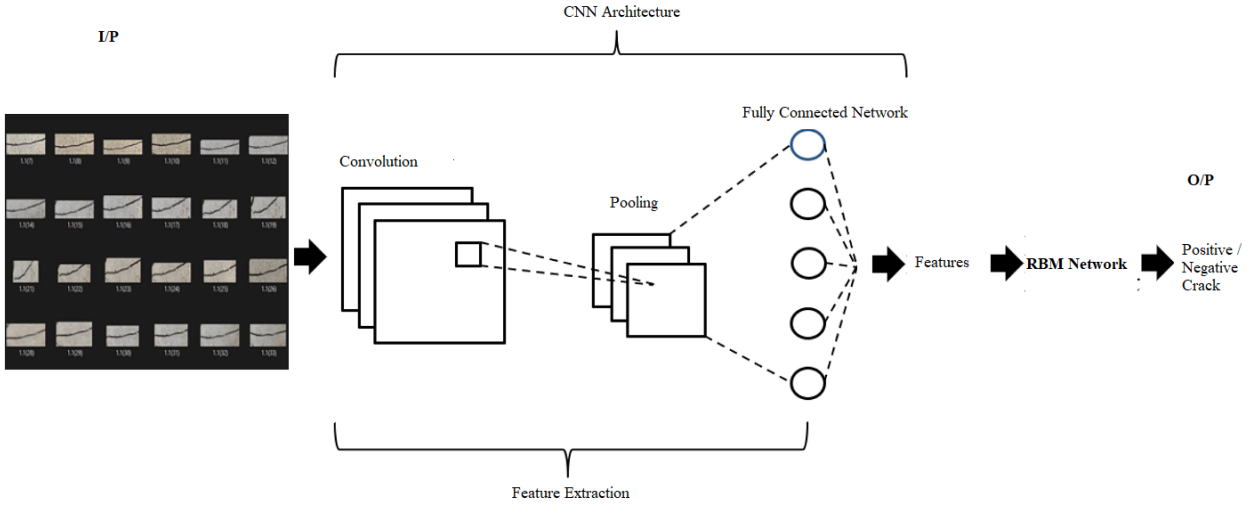

Figure 7. Integrated CNN model for crack prediction

3.2 Assumptions

DBN assumes that the hidden units within each layer are conditionally independent of the visible units. This assumption simplifies the modelling and learning process. DBN assumes the statistical properties of the data, and they remain constant across the layers. The assumptions may not always hold true, but even then, they simplify the learning process and enable effective feature learning.

Mathematically, the key equations governing the behaviour of a DBN involve the energy function and the conditional probabilities associated with each layer in an RBM. The joint probability distribution over visible units (v) and hidden units (h) is given by:

$$P(v,h) = \frac{1}{z} e^{-E(v,h)}$$

where, Z is the normalisation constant
$E(v,h)$ is the energy function defined as $-v^T W a - b^T v - c^T h$, where W is the weight matrix connecting visible and hidden units, a, b, and c are the biases for visible units, visible-to-hidden connections, and hidden units respectively.

The conditional probabilities are then calculated as:

$$P(h|v) = \frac{1}{1 + e^{-(W_{v+c})}}$$

$$P(v|h) = \frac{1}{1 + e^{(W^T{}_{h+c})}}$$

These equations govern the learning and inference processes in DBN.

Initially, the concrete surface images undergo segmentation, with each original image sliced into smaller patches using a sliding window. These patches, characterised by reduced pixel sizes, are then classified based on the actual surface conditions, distinguishing between intact and cracked areas. Following this, training and validation samples are randomly drawn from these categorised patches. These samples are then inputted into various CNN models, including AlexNet, DarkNet-19, DarkNet-53, DenseNet-201, EfficientNet-b0, GoogLeNet, Inception-v3, MobileNet-v2, ResNet-18, ResNet-50, ResNet-101, ShuffleNet, SqueezeNet, VGG-16, and VGG-19, for the initial recognition of surface conditions. These chosen CNNs are pretrained on the ImageNet dataset, with contains over a million images used for classifying a thousand objects. The Kaggle images [24] used in this experiment relate to structural engineering elements such as buildings, bridges, beams, columns, and walls, specifically focused on concrete crack images. Then, these CNNs that have already been trained on different deeper architectures are fine-tuned on new concrete surface image patches to turn them into models for finding crack patches.

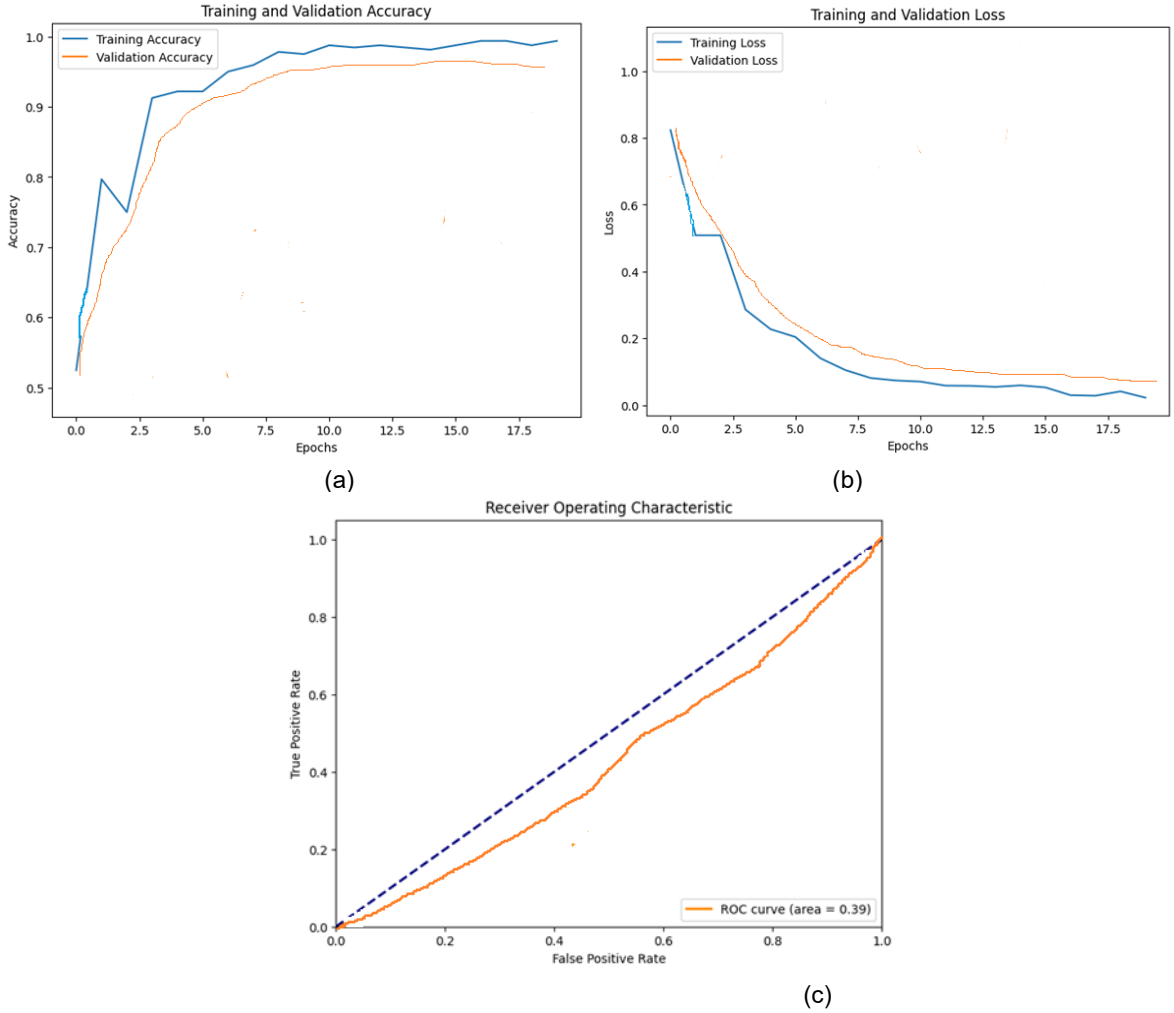

Figure 8. a) Training and validation accuracy b) Training and validation loss c) ROC curve

Differing from traditional networks that provide hard decisions, the CNNs in this study generate soft decisions, presenting probability values for all potential categories. As different network architectures exhibit varying capabilities for diagnosing concrete cracks, results from different CNN models may present conflicts. To address this, the proposed framework adopts a hierarchical configuration where the outputs of prior operations serve as inputs for subsequent operations. This approach significantly bolsters crack detection accuracy with a high level of confidence, leveraging multi-level information processing.

4 Results and discussion

To validate the effectiveness of the concrete crack prediction method utilising the deep belief network in real-world scenarios, a simulation experiment is conducted. The dataset was trained and validated using Python software. The program was executed in Google Colab for faster execution of a huge dataset and a large number of epochs.

Table 1: Number of images used for training and validation

Category	Training	Validation
With crack	3000	800
Without crack	3500	850

This research's primary innovation lies in the integration of deep learning-based Convolutional Neural Networks (CNNs), transfer learning through the deep belief algorithm, creating a hybridised model for predicting surface cracks in concrete structures. This model demonstrates superior predictive capabilities and robustness compared to existing deep learning methods. Additionally, the introduction of decision-level image fusion to concrete crack detection represents a novel aspect. This application significantly elevates the confidence level of prediction results, thereby further improving prediction accuracy. Equation (17-20) is used to measure the performance metrics of the parameters mentioned. Figure 8 depicts the curve for accuracy during training and validation of the dataset, the loss curve and the ROC curve, respectively.

$$\text{Sensitivity} = \frac{\text{TN}}{\text{TN} + \text{FP}} \tag{17}$$

$$\text{Precision} = \frac{\text{TP}}{\text{TP} + \text{FP}} \tag{18}$$

$$\text{NPV} = \frac{\text{TN}}{\text{TN} + \text{FN}} \tag{19}$$

$$\text{Accuracy} = \frac{\text{TP} + \text{TN}}{\text{TN} + \text{TP} + \text{FP} + \text{FN}} \tag{20}$$

Table 2. Comparison of accuracy and Area under curve (AUC) for different CNN models

Model Name	**Precision**	**Accuracy**	**F1 score**	**AUC**
DarkNet-51	97.55%	97.84%	95.78%	0.9292
ResNet-101	97.20%	97.51%	95.11%	0.9615
ShuffleNet	95.55%	97.82%	95.05%	0.9535
SqueezeNet	97.44%	97.11%	95.15%	0.9182
AlexNet	97.21%	97.57%	95.41%	0.9339
DarkNet-19	97.49%	97.72%	95.55%	0.9647
ResNet-50	97.27%	97.59%	95.47%	0.9311
GoogLeNet	97.57%	97.72%	95.71%	0.919
Inception-v1	97.18%	97.55%	95.19%	0.9063
MobileNet-v2	95.74%	97.41%	95.18%	0.8946
VGG-15	97.48%	97.98%	95.82%	0.9052
VGG-19	97.74%	97.98%	97.01%	0.8913
EfficentNet-b0	95.11%	98.05%	95.12%	0.9447
DenseNet-201	97.91%	97.41%	95.75%	0.9714
ResNet-18	95.70%	98.05%	95.10%	0.9734
Proposed	**98.29%**	**98.05%**	**97.51%**	**0.9796**

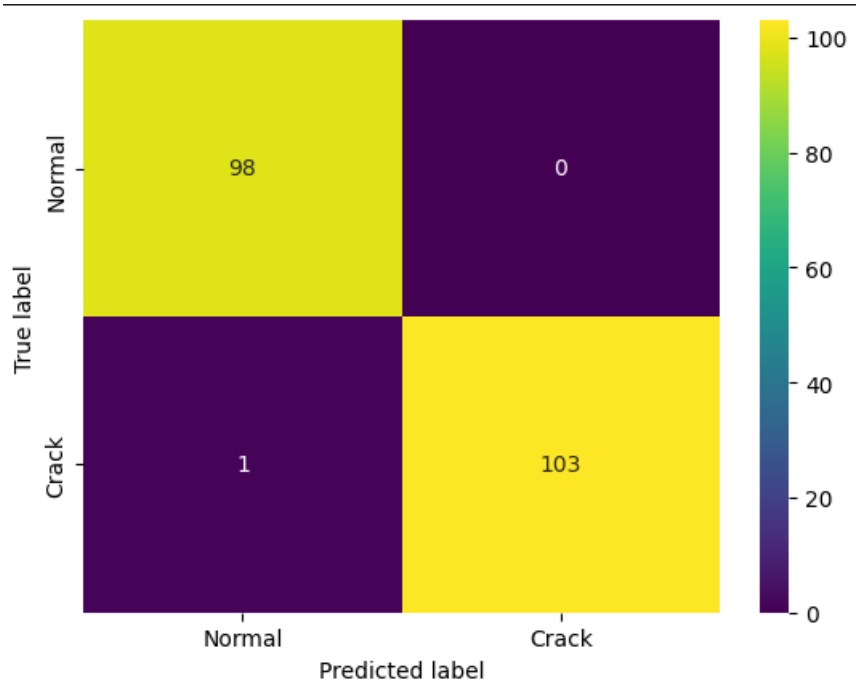

Figure 9. Confusion matrix for the proposed method

The proposed method has the highest values of metrics precision (98.29%), accuracy (98.05%), F1 score (97.51%), and AUC (0.9796). Figure 9 shows the confusion matrix.

4.1 Effects of Noise

In practical scenarios, images captured from the surfaces of concrete structures inevitably encounter various forms of contamination due to factors such as transmission channels and environmental conditions during acquisition and transmission. This results in the introduction of diverse noises, leading to information loss and distortion in the images. It is imperative to assess the resilience of the proposed method concerning crack patch detection in the presence of different types of noise. In pursuit of this objective, the study focuses on evaluating the robustness of the proposed method against two prevalent types of image noise: Salt and Pepper (SP) noise and Motion Blur (MB) noise. SP noise typically arises from improper ISO settings, while MB noise is a consequence of relative movement between the focal location and the camera. The evaluation indices of all the models are calculated after the test images undergo a noise removal process.

The study employed MATLAB software version 2021 installed on a PC with 16GB of RAM and 1TB of storage to incorporate noise effects into the concrete images. MATLAB is a widely used tool in the field of image processing due to its versatility and comprehensive set of functions tailored for handling and manipulating images.

5 Conclusion

The hybrid patch-based crack detection approach proposed in this study achieves an impressive identification accuracy of up to 97.7%. This notably outperforms both individual CNN models and the region-based crack detection method outlined in [25-27], which attains an optimal accuracy of 96%. So, the proposed method effectively fixes the problem of current crack detection models wrongly identifying cracks, which stops wrong estimates of the structure's remaining strength. The results presented in Figure 8, Figure 9, and Table 2 adequately demonstrate the effectiveness of the proposed hybridised method in concrete crack patch detection. The accuracy value and precision are almost 98% for the proposed DBN model. It rarely predicts a normal image as a concrete crack image, which is evident in the confusion matrix. Furthermore, this method is versatile; in addition to detecting surface cracks, it can also be employed to identify other types of structural defects, such as spalling, rebar exposure, corrosion, etc., provided corresponding images of structural defects are available for training. Even then, it is essential to note a significant drawback of the proposed method, which involves the rough estimation of crack area. This assumption is based on considering the size of the crack to be the same as the patch size.

The present study is subject to certain limitations. The models were specifically trained to identify and predict crack depths because of monotonic loading. There is a need for further investigations to validate the model's performance when confronted with cracks induced by different types of loading, such as cyclic loading. In addition to that, the models underwent training and testing using an image dataset characterised by a limited number of images. These images were captured under favourable lighting conditions, with efforts made to eliminate background noise. Future studies are encouraged to explore a broader range of illumination conditions and consider scenarios where background noise is present. It is worth noting that, in this study, the maximum crack depth was assumed to be uniform along the length of the crack. To address this simplification, further investigations are warranted to explore the actual variation in crack depth along the length of the crack. These refinements will contribute to a more comprehensive understanding of the model's applicability and performance across diverse conditions.

CRediT authorship contribution statement

Geetha R: Conceptualization, Methodology, Formal analysis,
Vijayalakshmi R: Investigation, Formal analysis, Writing – original draft.
Prakash R: Formal Analysis
Sathia R, Writing – original draft.

Declaration of Competing Interest

The authors declare that they have no known competing financial interests or personal relationships that could have appeared to influence the work reported in this paper.

Nomenclature

W_{cr}- Crack width as per IS 456-2000
a_{cr} - Distance considered from the point of the surface to the nearest longitudinal bar
ε_m - Average steel strain
C_{min} - Minimum cover of the longitudinal bar
$h(or)D$ - Overall depth of the member
x - Depth of the neutral axis
a -Distance from the compression face to point at which crack width is estimated
E_S- Modulus of elasticity of steel
$A_S(or)A_{St}$- Area of tension reinforcement
ε_1 - Strain at the level considered, calculation by ignoring concrete in the tension zone
b - Breadth of beam
d - Effective depth
m, n - Modular ratio
W_k - Design crack width as per BS EN1992-1-1-2004
ε_{sm} - Mean steel strain mostly under the effect of tension stiffening or shrinkage 0
ε_{cm} - Mean strain in concrete
f_s - Stress in tension reinforcement
k_t - Factor that expresses the duration of loading
$f_{ct,\,eff}$ - Mean value of tensile strength of the concrete
$A_{c,\,eff}$- Effective tension area
k_1- Coefficient which considers the bond properties of bonded reinforcement
k_2 - Coefficient strain distribution
Φ - Dia of bar
$S_{r,\,max}$ - Average stabilized crack spacing
ρ_{eff} - Effective reinforcement ratio
E_s - Modulus of elasticity for steel
E_c - Modulus of elasticity for concrete
C - Cover provided at the longitudinal bar
A_s - Area of tension reinforcement
W_k - Design crack width as per EGYPTIAN CODE; 203-2007
S_{rm} - Average stabilized crack spacing
β- Coefficient which is related to average crack width
β_1 - Coefficient for bar bond characteristics
β_2 - Coefficient which accounts load duration
f_{scr} - Stress in tension longitudinal reinforcement that causes under first crack stress in the tension reinforcement
d_c - Effective cover
M - Applied movement
I_{cr} - Moment of inertia for cracked section
W_{max}- Design crack width as per ACI 318-95
h - *Overall depth*
x - Depth of neutral axis
β - Coefficient relating the average crack width to the design value
A_o- Area of concrete surrounding each reinforcing bar

References

[1] W. Kaufmann, A. Amin, A. Beck, and M. Lee, “Shear transfer across cracks in steel fibre reinforced concrete,”. Eng Struct, 2019; Vol. 186:508–24.

[2] P. Folino, M. Ripani, H. Xargay, and N. Rocca,“Comprehensive analysis of fiber reinforced concrete beams with conventional reinforcement,” Eng Struct., 2020;202:109862.

[3] A. Bhosale, MA. Rasheed, SS. Prakash, and G. Raju, “A study on the efficiency of steel vs. synthetic vs. hybrid fibers on fracture behaviour of concrete in flexure using acoustic emission,” Constr Build Mater 2019;199:256–68.

[4] R. Sathia and R. Vijayalakshmi, “Fresh and mechanical property of caryota-urens fiber reinforced flowable concrete,” J. Mater. Res. Technol., vol. 15, pp. 3647–3662, 2021, doi: 10.1016/j.jmrt.2021.09.126.

[5] R. Vijayalakshmi et al., “Fresh and Hardened Property of Fish Tail Palm Fiber Reinforced concrete - Effect ofFiber Content and Fiber Length,” Eur. J. Environ. Civ. Eng., pp. 1–19, 2022, [Online]. Available: https://doi.org/10.1080/19648189.2022.2086178.

[6] B. Bhosale, C. Lakavath, and S. Suriya Prakash, “Multi-linear tensile stress-crack width relationships for hybrid fibre reinforced concrete using inverse analysis and digital image correlation,” Eng. Struct., vol. 225, no. February, p. 111275, 2020, doi: 10.1016/j.engstruct.2020.111275.

[7] S. Mansourdehghan, K.M. Dolatshahi, A.H. Asjodi, Data-driven damage assessment of reinforced concrete shear walls using visual features of damage, J. Build. Eng. (2022), 104509.

[8] H. Kim, E. Ahn, S. Cho, M. Shin, S.H. Sim, Comparative analysis of image binarization methods for crack identification in concrete structures, Cement Concr.Res. 99 (2017) 53–61.

[9] M. Rabah, A. Elhattab, A. Fayad, Automatic concrete cracks detection and mapping of terrestrial laser scan data, NRIAG J. Astron.Geophys. 2 (2) (2013) 250–255.

[10] T. Yamaguchi, S. Nakamura, R. Saegusa, S. Hashimoto, Image-based crack detection for real concrete surfaces, IEEJ Trans. Electr. Electron. Eng. 3 (1) (2008) 128–135.

[11] B.Y. Lee, Y.Y. Kim, S.-T. Yi, J.-K. Kim, Automated image processing technique for detecting and analysing concrete surface cracks, Struct. Infrastruct. Eng. 9 (6) (2013) 567–577.

[12] G. Li, X. Zhao, K. Du, F. Ru, Y. Zhang, Recognition and evaluation of bridge cracks with modified active contour model and greedy search-based support vector machine, Autom. ConStruct. 78 (2017) 51–61.

[13] M.R. Jahanshahi, S.F. Masri, C.W. Padgett, G.S. Sukhatme, An innovative methodology for detection and quantification of cracks through incorporation of depth perception, Mach. Vis. Appl. 24 (2) (2013) 227–241.

[14] C.V. Dung, “Autonomous concrete crack detection using deep fully convolutional neural network,”. Autom. Constr. 2019, 99, 52–58

[15] Sandeep Sony, Kyle Dunphy, Ayan Sadhu, Miriam Capretz, A systematic review of convolutional neural network-based structural condition assessment techniques, Engineering Structures, Volume 226, 2021, 111347, ISSN 0141-0296.

[16] D. Li, J. Liu, S. Hu, G. Cheng, Y. Li, Y. Cao, B. Dong, Y.F. Chen, A deep learning-based indoor acceptance system for assessment on flatness and verticality quality of concrete surfaces, J. Build. Eng. 51 (2022), 104284.

[17] Y. Xu, S. Li, D. Zhang, Y. Jin, F. Zhang, N. Li, H. Li, Identification framework for cracks on a steel structure surface by a restricted Boltzmann machines algorithm based on consumer-grade camera images, Struct. Control Health Monit. 25 (2) (2018), e2075.

[18] C. Modarres, N. Astorga, E.L. Droguett, V. Meruane, Convolutional neural networks for automated damage recognition and damage type identification, Struct. Control Health Monit. 25 (10) (2018), e2230.

[19] J. Jo, Z. Jadidi, A high precision crack classification system using multi-layered image processing and deep belief learning, Struct. Infrastruct. Eng. 16 (2) (2020) 297–305.

[20] S. Li, X. Zhao, Image-based concrete crack detection using convolutional neural network and exhaustive search technique, Adv. Civ. Eng. (2019) 2019.

[21] F.-C. Chen, M.R. Jahanshahi, NB-CNN, Deep learning-based crack detection using convolutional neural network and Naïve Bayes data fusion, IEEE Trans. Ind. Electron. 65 (5) (2017) 4392–4400.

[22] F. Fang, L. Li, Y. Gu, H. Zhu, J.-H. Lim, A novel hybrid approach for crack detection, Pattern Recogn. 107 (2020), 107474.

[23] A. Krizhevsky, I. Sutskever, G.E. Hinton, Imagenet classification with deep convolutional neural networks, Adv. Neural Inf. Process. Syst. 25 (2012) 1097–1105.

[24] C.F. Ozgenel, (2019), “Concrete Crack Images for Classification”, Mendeley Data, V2, doi: 10.17632/5y9wdsg2zt.2

[25] K. Simonyan, A. Zisserman, Very Deep Convolutional Networks for Large-Scale Image Recognition, 2014, p. 1556, arXiv preprint arXiv:1409.

[26] S.J. Pan, Q. Yang, A survey on transfer learning, IEEE Trans. Knowl. Data Eng. 22 (10) (2009) 1345–1359.

[27] .S. Rao, T. Nguyen, M. Palaniswami, T. Ngo, Vision-based Automated Crack Detection Using Convolutional Neural Networks for Condition Assessment of Infrastructure, Structural Health Monitoring, 2020, 1475921720965445.